AIP Applied Physics Letters

Effect of excited states on the ground-state modulation bandwidth in quantum dot lasers

Yuchang Wu, Robert A. Suris, and Levon V. Asryan

Citation: Applied Physics Letters **102**, 191102 (2013); doi: 10.1063/1.4804994
View online: http://dx.doi.org/10.1063/1.4804994
View Table of Contents: http://scitation.aip.org/content/aip/journal/apl/102/19?ver=pdfcov
Published by the AIP Publishing

Effect of excited states on the ground-state modulation bandwidth in quantum dot lasers

Yuchang Wu,[1,a)] Robert A. Suris,[2,b)] and Levon V. Asryan[1,c)]
[1]*Virginia Polytechnic Institute and State University, Blacksburg, Virginia 24061, USA*
[2]*Ioffe Physico-Technical Institute, St. Petersburg 194021, Russia*

(Received 10 February 2013; accepted 29 April 2013; published online 13 May 2013)

We consider direct and indirect (excited-state-mediated) capture of carriers from the waveguide region into the lasing ground state in quantum dots (QDs) and calculate the modulation response of a QD laser. We show that, when only indirect capture is involved, the excited-to-ground-state relaxation delay strongly limits the ground-state modulation bandwidth of the laser—at the longest tolerable relaxation time, the bandwidth becomes zero. When direct capture is also involved, the effect of excited-to-ground-state relaxation is less significant and the modulation bandwidth is considerably higher. © *2013 AIP Publishing LLC*. [http://dx.doi.org/10.1063/1.4804994]

In Ref. 1, the upper limit for the small-signal modulation bandwidth ideally attainable in quantum dot (QD) lasers was estimated. The experimental modulation bandwidth in QD lasers[2,3] is actually considerably lower. Several factors can affect the dynamic properties of QD lasers and limit the modulation bandwidth. Among such factors are the carrier capture delay from the higher-dimensionality reservoir regions (2D wetting layer[4–7] and bulk optical confinement layer (OCL)[8]) into QDs, the internal optical loss, which increases with carrier density in the OCL,[9] and the gain compression (see, e.g., Ref. 10).

In this letter, we report on the effect of excited states, which are typically present in QDs,[11,12] on the ground-state modulation response of a QD laser. Recombination processes via excited states (Fig. 1) reduce the efficiency of carrier injection into the ground state in QDs (Fig. 1). In this regard, the role of recombination via excited states in QDs is similar to that of parasitic recombination in the OCL[13] (Fig. 1). There is also relaxation delay from the excited- to ground-state in a QD.[14–22] Under the conditions of a two-step (excited-state-mediated) capture from the OCL into the QD ground-state, the excited-to-ground-state relaxation delay will be added to the OCL-to-excited-state capture delay.

In Refs. 4, 5, and 8, the effect of carrier capture delay from the reservoir into single-level QDs (i.e., into the QD ground-state) on the modulation bandwidth was studied. In Refs. 6 and 7, the effect of capture delay from the reservoir into the QD excited-state on the ground-state modulation response was discussed. While the capture delays from the reservoir into both the QD ground- and excited-states are inherently included in the model of the present work, the primary focus here is the effect of excited-to-ground-state relaxation delay inside QDs on the ground-state modulation bandwidth.

Our theoretical model is illustrated in Fig. 1. The carriers injected in the OCL can be either directly captured into the QD ground-state or first captured into the excited state and then relax to the ground state. The carriers localized in QDs can escape back to the OCL. For the carriers localized in the ground state, the escape process can be either direct or via the excited state. We used the detailed balance condition to derive the relationship between the time τ_{12} of upward transitions from the ground- to excited-state and the time τ_{21} of relaxation from the excited- to ground-state. The relation reads as $\tau_{12} = \tau_{21}\exp[(E_{n1} - E_{n2})/T]$, where E_{n1} and E_{n2} are the energies of carrier excitation from the QD ground- and excited-state to the OCL (see Fig. 1), and T is the temperature (in units of energy). The spontaneous radiative recombination occurs via the OCL states and both the ground- and excited-states in QDs. Since the focus of this work is the effect of carrier relaxation to the lasing state on the modulation bandwidth, we restrict our consideration to stimulated emission only via the QD ground-state. The case of lasing via the upper excited-state is not essentially different from the case of single-level QDs considered in Ref. 8.

With the above processes included in our model, we have the following set of four coupled rate equations for free carriers in the OCL, carriers confined in the QD excited-state, those confined in the QD ground-state, and photons:

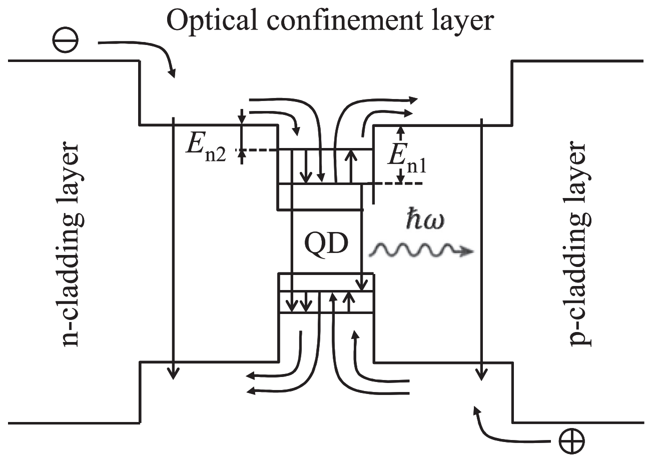

FIG. 1. Energy band diagram of a QD laser. One excited state is assumed for each type of carriers in QDs in addition to the ground state. Both direct and indirect (excited-state-mediated) capture processes into the lasing ground state are considered.

a)Electronic mail: yuchangw@vt.edu
b)Electronic mail: suris@theory.ioffe.ru
c)Electronic mail: asryan@vt.edu

$$\frac{\partial n_{\rm OCL}}{\partial t}=\frac{j}{eb}-\sigma_{\rm n2}{\rm v_n}\frac{N_{\rm S}}{b}(1-f_{\rm n2})n_{\rm OCL}+\sigma_{\rm n2}{\rm v_n}n_2\frac{N_{\rm S}}{b}f_{\rm n2}-\sigma_{\rm n1}{\rm v_n}\frac{N_{\rm S}}{b}(1-f_{\rm n1})n_{\rm OCL}+\sigma_{\rm n1}{\rm v_n}n_1\frac{N_{\rm S}}{b}f_{\rm n1}-Bn_{\rm OCL}^2, \quad (1)$$

$$\frac{\partial}{\partial t}\left(2\frac{N_{\rm S}}{b}f_{\rm n2}\right)=\sigma_{\rm n2}{\rm v_n}\frac{N_{\rm S}}{b}(1-f_{\rm n2})n_{\rm OCL}-\sigma_{\rm n2}{\rm v_n}n_2\frac{N_{\rm S}}{b}f_{\rm n2}+\frac{N_{\rm S}}{b}\frac{f_{\rm n1}(1-f_{\rm n2})}{\tau_{12}}-\frac{N_{\rm S}}{b}\frac{f_{\rm n2}(1-f_{\rm n1})}{\tau_{21}}-\frac{N_{\rm S}}{b}\frac{f_{\rm n2}^2}{\tau_{\rm QD2}}, \quad (2)$$

$$\begin{aligned}\frac{\partial}{\partial t}\left(2\frac{N_{\rm S}}{b}f_{\rm n1}\right)=&\ \sigma_{\rm n1}{\rm v_n}\frac{N_{\rm S}}{b}(1-f_{\rm n1})n_{\rm OCL}-\sigma_{\rm n1}{\rm v_n}n_1\frac{N_{\rm S}}{b}f_{\rm n1}+\frac{N_{\rm S}}{b}\frac{f_{\rm n2}(1-f_{\rm n1})}{\tau_{21}}\\ &-\frac{N_{\rm S}}{b}\frac{f_{\rm n1}(1-f_{\rm n2})}{\tau_{12}}-\frac{N_{\rm S}}{b}\frac{f_{\rm n1}^2}{\tau_{\rm QD1}}-{\rm v_g}g_1^{\rm max}(2f_{\rm n1}-1)n_{\rm ph},\end{aligned} \quad (3)$$

$$\frac{\partial n_{\rm ph}}{\partial t}={\rm v_g}g_1^{\rm max}(2f_{\rm n1}-1)n_{\rm ph}-{\rm v_g}\beta n_{\rm ph}, \quad (4)$$

where $n_{\rm OCL}$ is the free carrier density in the OCL, $f_{\rm n1}$ and $f_{\rm n2}$ are the occupancies of the ground- and excited-state in a QD, and $n_{\rm ph}$ is the photon density (per unit volume of the OCL) in the lasing mode. The other parameters are as follows: j is the injection current density, b is the OCL thickness, $\sigma_{\rm n1}$ and $\sigma_{\rm n2}$ are the cross-sections of carrier capture from the OCL into the QD ground- and excited-state, ${\rm v_n}$ is the free carrier thermal velocity in the OCL, $N_{\rm S}$ is the total surface density of QDs (the product of the number of layers with QDs and the surface density of QDs in a single-layer), B is the spontaneous radiative recombination constant for the OCL, $\tau_{\rm QD1}$ and $\tau_{\rm QD2}$ are the spontaneous radiative recombination lifetimes via the QD ground- and excited-state, $g_1^{\rm max}$ is the maximum modal gain for the ground-state transitions ($g_1^{\rm max}$ increases directly with $N_{\rm S}$—see Refs. 26 and 28), $\beta=(1/L)\ln(1/R)$ is the mirror loss, L is the cavity length, and R is the facet reflectivity.

The quantities $n_1=N_{\rm c}^{\rm 3D}\exp(-E_{\rm n1}/T)$ and $n_2=N_{\rm c}^{\rm 3D}\exp(-E_{\rm n2}/T)$ characterize the intensities of thermal escapes from the QD ground- and excited-state to the OCL (Fig. 1), where $N_{\rm c}^{\rm 3D}$ is the effective density of states in the OCL.

As in Refs. 4, 5, and 8, our model does not include the fraction of spontaneous emission entering the lasing mode. This fraction is generally very small,[23] and this is the more so in QD lasers, since the spontaneous emission rate in QDs is itself low. Even slightly above the lasing threshold, the fraction of spontaneous emission is negligible as compared to the stimulated emission rate. Neglecting this fraction makes our analysis and derivations simpler while not considerably influencing the physical picture.

We consider a direct modulation of the laser output by the small time-harmonic component δj of the pump current density j and, correspondingly, use the small-signal analysis[23–25] of rate equations (1)–(4). Looking for the solutions of the rate equations in the form of the sum of the dc (steady-state) component and the small time-harmonic component, we arrive at the set of algebraic equations in the small frequency-dependent amplitudes $\delta n_{\rm OCL-m}$, $\delta f_{\rm n1-m}$, $\delta f_{\rm n2-m}$, and $\delta n_{\rm ph-m}$. From the solution of this set, we find the ratio

$$\frac{\delta n_{\rm ph-m}(\omega)}{\delta n_{\rm ph-m}(0)}=\frac{A_0}{(\omega^4-A_2\omega^2+A_0)-i\,(A_3\omega^3-A_1\omega)}, \quad (5)$$

where ω is the angular frequency of modulation. The modulation response function is calculated as $H(\omega)=|\delta n_{\rm ph-m}(\omega)/\delta n_{\rm ph-m}(0)|^2$. The coefficients A_1, A_2, and A_3 are positive; A_0 is positive above the lasing threshold and zero at and below the lasing threshold. They are functions of the dc component j_0 of the injection current density and parameters of the laser structure. The expressions for these coefficients are cumbersome and not presented here for reasons of space.

We obtain the following quartic equation for the square of the modulation bandwidth $\omega_{-3\,\rm dB}$ [the frequency, at which $H(\omega)$ has fallen to half its dc ($\omega=0$) value: $10\log_{10}H(\omega_{-3\,\rm dB})=-3$]:

$$\begin{aligned}&\omega_{-3\,\rm dB}^8+(A_3^2-2A_2)\omega_{-3\,\rm dB}^6+(A_2^2+2A_0-2A_1A_3)\omega_{-3\,\rm dB}^4\\&+(A_1^2-2A_0A_2)\omega_{-3\,\rm dB}^2-(r-1)A_0^2=0,\end{aligned} \quad (6)$$

where the numerical parameter $r=10^{0.3}\approx 1.995$.

The analysis of Eq. (6) shows that, under the lasing condition, i.e., if the dc component of the pump current density is above the threshold current density ($j_0>j_{\rm th}$), only one out of four roots $\omega_{-3\,\rm dB}^2$ of Eq. (6) is positive and hence physically meaningful. At the lasing threshold ($j_0=j_{\rm th}$), this root $\omega_{-3\,\rm dB}^2$ becomes zero (Fig. 2); at a small excess of j_0 above $j_{\rm th}$, $\omega_{-3\,\rm dB}^2\propto(j_0-j_{\rm th})^2$ and hence

$$\omega_{-3\,\rm dB}\propto j_0-j_{\rm th}. \quad (7)$$

For $j_0<j_{\rm th}$ (below the lasing threshold), Eq. (6) does not have any positive root $\omega_{-3\,\rm dB}^2$.

Below, we discuss the dependences of the modulation bandwidth $\omega_{-3\,\rm dB}$ on j_0 and parameters of the structure. We consider a GaInAsP heterostructure lasing near 1.55 μm at room-temperature.[26,27] In a single-QD-layer structure, the maximum gain for the ground-state transitions $g_1^{\rm max}=29.52\,{\rm cm}^{-1}$, which corresponds to 10% QD-size fluctuations, the surface density of QDs in a layer $6.11\times10^{10}\,{\rm cm}^{-2}$, and an ideal overlap between the electron and hole ground-state wave functions.[28] The mirror loss $\beta=10\,{\rm cm}^{-1}$ (at the as-cleaved facet reflectivity $R=0.32$, this corresponds to the

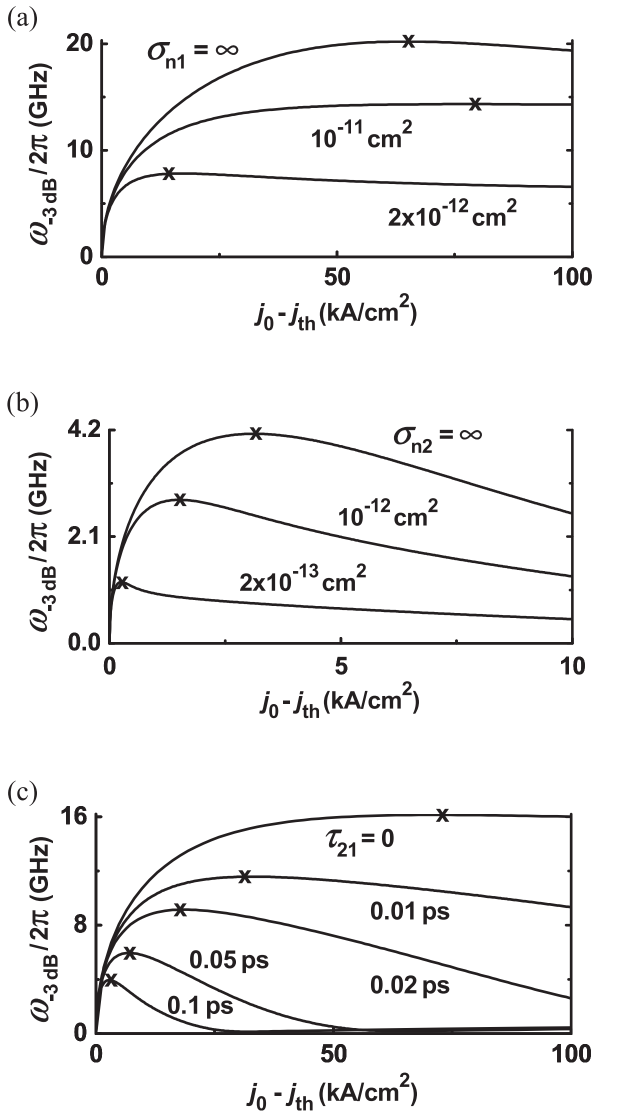

FIG. 2. Modulation bandwidth $\omega_{-3\,\mathrm{dB}}/2\pi$ vs. excess of the dc component of the injection current density over the threshold current density. In (a), $\sigma_{n2} = 10^{-11}\,\mathrm{cm}^2$, $\tau_{21} = 0.1$ ps, and σ_{n1} is different for different curves; $\sigma_{n1} = \infty$ corresponds to instantaneous carrier exchange between the OCL and the QD ground-state. In (b), $\sigma_{n1} = 0$ (no direct capture into the QD ground-state), $\tau_{21} = 0.1$ ps, and σ_{n2} is different for different curves; $\sigma_{n2} = \infty$ corresponds to instantaneous exchange between the OCL and the QD excited-state. In (c), $\sigma_{n1} = 0$ (no direct capture into the QD ground-state), $\sigma_{n2} = 10^{-11}$ cm^2, and τ_{21} is different for different curves; $\tau_{21} = 0$ corresponds to instantaneous exchange between the QD excited- and ground-state. Throughout the paper, the cavity length $L = 1.139$ mm is assumed (the mirror loss $\beta = 10\,\mathrm{cm}^{-1}$). The symbol "×" marks the maximum modulation bandwidth $\omega^{\max}_{-3\,\mathrm{dB}}/2\pi$ on each curve.

cavity length $L = 1.139$ mm) and the OCL thickness $b = 0.28\,\mu$m.

Figure 2 shows the modulation bandwidth against excess of j_0 over j_{th}. As seen from the figure, with j_0 increasing from j_{th}, $\omega_{-3\,\mathrm{dB}}$ increases from zero, approaches its maximum value $\omega^{\max}_{-3\,\mathrm{dB}}$ (marked by the symbol "×") at a certain optimum value of j_0, and then decreases.

In the presence of fast direct capture into the ground state (when σ_{n1} is large), $\omega_{-3\,\mathrm{dB}}$ is mainly controlled by σ_{n1} and only slightly affected by σ_{n2} and τ_{21}. In Fig. 2(a), the cross-section σ_{n2} of capture from the OCL into the QD excited-state and the excited-to-ground-state relaxation time τ_{21} are fixed while the capture cross-section σ_{n1} into the ground state

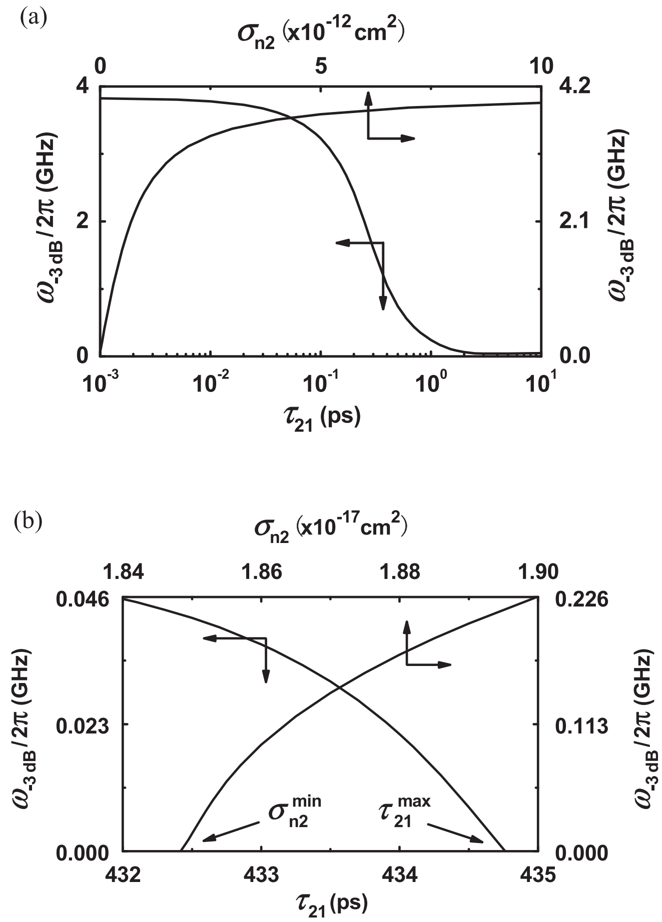

FIG. 3. Modulation bandwidth $\omega_{-3\,\mathrm{dB}}/2\pi$ vs. capture cross-section into the QD excited-state (at $j_0 = 3\,\mathrm{kA/cm}^2$ and $\tau_{21} = 0.1$ ps) and excited-to-ground-state relaxation time (at $j_0 = 1\,\mathrm{kA/cm}^2$ and $\sigma_{n2} = 10^{-11}$ cm^2) for the case of no direct capture into the QD ground-state ($\sigma_{n1} = 0$). In (b), the portions of the curves near the minimum tolerable value $\sigma^{\min}_{n2}$ of σ_{n2} and the maximum tolerable value $\tau^{\max}_{21}$ of τ_{21} are shown.

is different for different curves. As seen from the figure, with reducing σ_{n1} (i.e., making slower the capture to the ground state), $\omega_{-3\,\mathrm{dB}}$ decreases.

Making slower the excited-state-mediated capture into the lasing ground-state (i.e., decreasing σ_{n2} and/or increasing τ_{21}) also reduces the modulation bandwidth. However, only

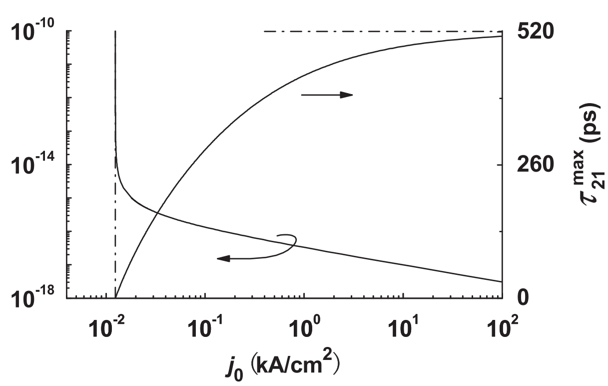

FIG. 4. Minimum tolerable value $\sigma^{\min}_{n2}$ of the capture cross-section into the QD excited-state (at $\tau_{21} = 0.1$ ps) and maximum tolerable value $\tau^{\max}_{21}$ of the excited-to-ground-state relaxation time (at $\sigma_{n2} = 10^{-11}$ cm^2) vs. dc component of the injection current density. No direct capture into the QD ground-state is involved ($\sigma_{n1} = 0$). The vertical dashed-dotted line marks the value $j_0 = j_{\mathrm{th},\,\sigma_{n2}=\infty}$. The horizontal dashed-dotted line marks the saturation value of $\tau^{\max}_{21}$ at $j_0 \to \infty$ given by Eq. (9).

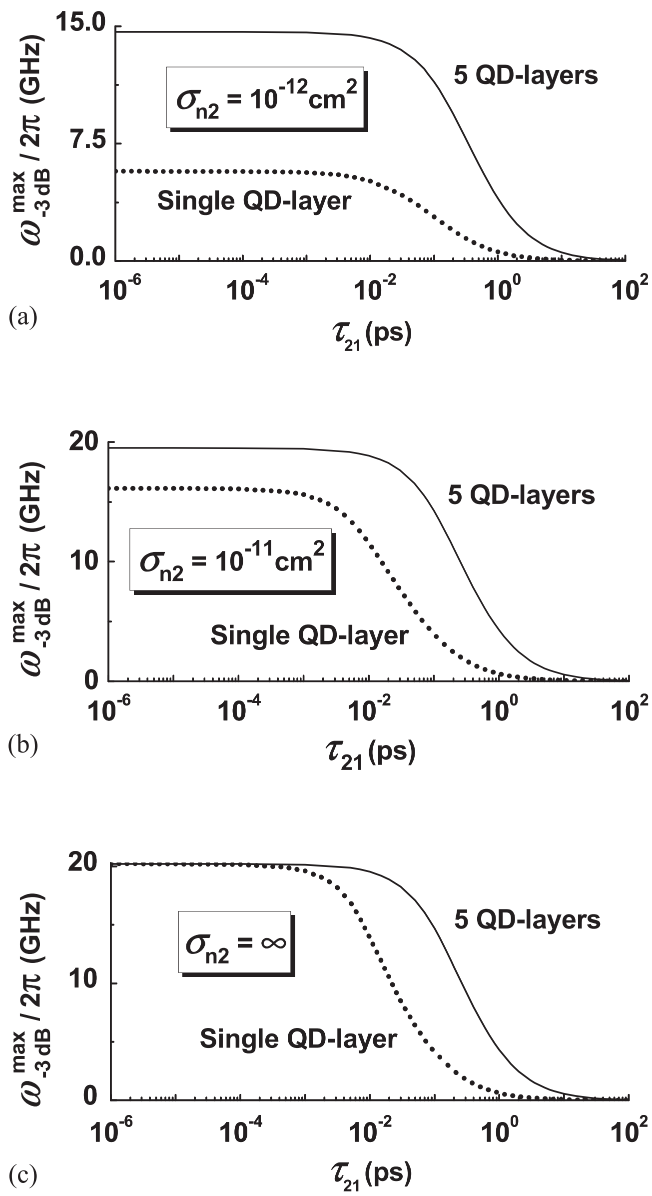

FIG. 5. Maximum modulation bandwidth $\omega_{-3\,dB}^{max}/2\pi$ (maximum of the dependence of $\omega_{-3\,dB}/2\pi$ on j_0—see Fig. 2) vs. excited-to-ground-state relaxation time for a single- and a 5-QD-layer structures at different values of the capture cross-section σ_{n2} into the QD excited-state: (a) $\sigma_{n2} = 10^{-12}$ cm^2, (b) $\sigma_{n2} = 10^{-11}$ cm^2, and (c) $\sigma_{n2} = \infty$. For both structures, $L = 1.139$ mm and no direct capture into the QD ground-state is involved ($\sigma_{n1} = 0$).

when σ_{n1} is small, the effect of σ_{n2} and τ_{21} on $\omega_{-3\ dB}$ becomes stronger. The modulation bandwidth is particularly strongly affected by σ_{n2} and τ_{21} when there is no direct capture from the OCL into the QD ground-state, i.e., $\sigma_{n1} = 0$ [Figs. 2(b), 2(c), and 3–5]. In Fig. 2(b), τ_{21} is fixed while σ_{n2} is different for different curves. In Fig. 2(c), σ_{n2} is fixed while τ_{21} is different for different curves.

As seen from Figs. 2(b), 2(c), and 3, in such a case of no direct capture, the modulation bandwidth drops rapidly with decreasing capture cross-section σ_{n2} or increasing relaxation time τ_{21}. Even at a short relaxation time of 0.1 ps, the maximum modulation bandwidth (4 GHz) is four times lower than that at instantaneous relaxation (16 GHz at $\tau_{21} = 0$)—see Figs. 2(c) and 5.

It is seen from Fig. 3(b) that there exist the minimum tolerable value σ_{n2}^{min} of σ_{n2} and the maximum tolerable value τ_{21}^{max} of τ_{21} at which $\omega_{-3\ dB}$ becomes zero. The point is that, for lasing to occur and for direct modulation of laser output, the dc component j_0 of the pump current density should be higher than the threshold current density j_{th}. With decreasing σ_{n2} or increasing τ_{21}, the threshold current density increases. It is at $\sigma_{n2} = \sigma_{n2}^{min}$ or $\tau_{21} = \tau_{21}^{max}$ when j_{th} becomes equal to j_0. The following expression is obtained for σ_{n2}^{min} from the condition $j_{th} = j_0$:

$$\sigma_{n2}^{min} = \frac{1}{v_n}\frac{1}{1-f_{n2\_th}}\frac{j_{th}^{QD}}{eN_S}\sqrt{ebB} \times \frac{\sqrt{j_0 - j_{th}^{QD}} + \sqrt{j_{th,\,\sigma_{n2}=\infty} - j_{th}^{QD}}}{j_0 - j_{th,\,\sigma_{n2}=\infty}}, \quad (8)$$

where f_{n2_th} is the excited-state level occupancy at the lasing threshold, j_{th}^{QD} is the component of j_{th} associated with the spontaneous recombination in QDs, and $j_{th,\,\sigma_{n2}=\infty}$ is the threshold current density for the case of instantaneous capture into the excited state ($\sigma_{n2} = \infty$). The same condition $j_{th} = j_0$ should be used to calculate τ_{21}^{max} but no closed-form expression can be derived for τ_{21}^{max}.

As seen from Eq. (8) and Fig. 4, σ_{n2}^{min} depends strongly on j_0. At $j_0 \to j_{th,\,\sigma_{n2}=\infty}$ (the vertical dashed-dotted line in the figure), $\sigma_{n2}^{min} \to \infty$. The higher is j_0, the smaller is σ_{n2}^{min}.

The longest relaxation time τ_{21}^{max} also depends strongly on j_0 (Fig. 4). τ_{21}^{max} is zero at $j_0 = j_{th,\,\tau_{21}=0}$ (the difference between $j_{th,\,\tau_{21}=0}$ and $j_{th,\,\sigma_{n2}=\infty}$ is very small and cannot be seen in Fig. 4). τ_{21}^{max} increases with j_0 and saturates at the value (the horizontal dashed-dotted line)

$$\tau_{21}^{max}|_{j_0\to\infty} = \frac{1-f_{n1,0}}{f_{n1,0}^2}\tau_{QD1}, \quad (9)$$

where $f_{n1,0}$ is the steady-state (dc) occupancy of the QD ground-state, which is pinned above the lasing threshold (does not change with j_0) and given by

$$f_{n1,0} = \frac{1}{2}\left(1 + \frac{\beta}{g_1^{max}}\right). \quad (10)$$

It is clear from the above discussion that, if the abscissa and the ordinate are interchanged in Fig. 4, we will obtain the threshold current density j_{th} against σ_{n2} and τ_{21}.

For the case of no direct capture into the QD ground-state, Fig. 5 shows the dependence of the maximum modulation bandwidth $\omega_{-3\ dB}^{max}$ on τ_{21}. To obtain this dependence, we calculated the modulation bandwidth $\omega_{-3\ dB}$ as a function of the dc component j_0 of the injection current density at different values of τ_{21} [Fig. 2(c)]; we then determined for each τ_{21} the corresponding maximum value $\omega_{-3\ dB}^{max}$ [marked by the symbol "×" in Fig. 2(c)] of the function $\omega_{-3\,dB}(j_0)$. For comparison, single- and 5-QD-layer structures are considered and three different values of σ_{n2} are used in the figure. As seen from the figure, with reducing τ_{21}, $\omega_{-3\ dB}^{max}$ increases and saturates. The saturation value of $\omega_{-3\ dB}^{max}$ corresponds to the case of instantaneous excited-to-ground-state relaxation in QDs ($\tau_{21} = 0$). At a finite value of σ_{n2} [10^{-12} and 10^{-11} cm^2 in (a) and (b), respectively], i.e., at noninstantaneous capture from the OCL into the QD excited-state, the saturation value in a 5-layer structure is higher than that in a single-layer structure [14.6 vs. 5.7 GHz in (a) and 19.5 vs. 16.1 GHz in (b)]. The difference in $\omega_{-3\ \mathrm{dB}}^{\max}$ between a 5- and a single-layer-structure becomes larger at noninstantaneous relaxation—it is considerable [9.4 vs. 1.9 GHz in (a), 11.2 vs. 2.4 GHz in (b), and 11.4 vs. 2.5 GHz in (c)] already at a short relaxation time $\tau_{21} = 0.2$ ps. The physical mechanism behind the enhancement of $\omega_{-3\ \mathrm{dB}}^{\max}$ in a multi-layer structure is similar to the case of single-level QDs[8]—with increasing N_s (i.e., number of QD layers and/or surface density of QDs in a single-layer), the carrier exchange [either direct or excited-state-mediated—see the second through fifth terms in the right-hand side of Eq. (1)] between the OCL and the lasing ground state in QDs becomes faster.

In going from (a) to (b) and then to (c) in Fig. 5, i.e., with increasing σ_{n2}, the saturation values of $\omega_{-3\ \mathrm{dB}}^{\max}$ in 5- and single-layer structures increase and become closer to each other. At $\sigma_{n2} = \infty$ [Fig. 5(c)], i.e., at instantaneous capture from the OCL into the QD excited-state, the saturation values in 5- and single-layer structures become the same (20.2 GHz).

In conclusion, we have considered direct and excited-state-mediated capture of carriers from the OCL into the lasing ground state in QDs and calculated the modulation response of a QD laser. We have shown that, when only indirect capture is involved, the delays in the carrier capture from the OCL into the QD excited-state and in excited-to-ground-state relaxation strongly limit the modulation bandwidth $\omega_{-3\ \mathrm{dB}}$ of the laser—at the minimum tolerable capture cross-section or longest relaxation time, $\omega_{-3\ \mathrm{dB}}$ becomes zero. When a fast direct capture is also involved, the modulation bandwidth is considerably higher and only slightly affected by the presence of excited states. The effect of excited states is also less significant and $\omega_{-3\ \mathrm{dB}}$ is higher in multi-QD-layer structures as compared to a single-layer structure.

L.V.A. and Y.W. acknowledge the U.S. Army Research Office (Grant No. W911-NF-08-1-0462), Y.W. also acknowledges the China Scholarship Council, and R.A.S. acknowledges the Russian Foundation for Basic Research (Grant No. 11-02-00573) and the Program "Fundamental Research in Nanotechnology and Nanomaterials" of the Presidium of the Russian Academy of Sciences for support of this work.

[1] L. V. Asryan and R. A. Suris, Appl. Phys. Lett. **96**, 221112 (2010).
[2] K. Kamath, J. Phillips, H. Jiang, J. Singh, and P. Bhattacharya, Appl. Phys. Lett. **70**, 2952 (1997).
[3] S. Fathpour, Z. Mi, and P. Bhattacharya, J. Phys. D: Appl. Phys. **38**, 2103 (2005).
[4] M. Ishida, N. Hatori, T. Akiyama, K. Otsubo, Y. Nakata, H. Ebe, M. Sugawara, and Y. Arakawa, Appl. Phys. Lett. **85**, 4145 (2004).
[5] M. Ishida, M. Sugawara, T. Yamamoto, N. Hatori, H. Ebe, Y. Nakata, and Y. Arakawa, J. Appl. Phys. **101**, 013108 (2007).
[6] D. G. Deppe and H. Huang, IEEE J. Quantum Electron. **42**, 324 (2006).
[7] D. G. Deppe and D. L. Huffaker, Appl. Phys. Lett. **77**, 3325 (2000).
[8] L. V. Asryan, Y. Wu, and R. A. Suris, Appl. Phys. Lett. **98**, 131108 (2011).
[9] Y. Wu, R. A. Suris, and L. V. Asryan, Appl. Phys. Lett. **100**, 131106 (2012).
[10] A. E. Zhukov, M. V. Maksimov, and A. R. Kovsh, Semiconductors **46**, 1225 (2012).
[11] L. W. Wang, J. N. Kim, and A. Zunger, Phys. Rev. B **59**, 5678 (1999).
[12] O. Stier, M. Grundmann, and D. Bimberg, Phys. Rev. B **59**, 5688 (1999).
[13] L. V. Asryan, S. Luryi, and R. A. Suris, Appl. Phys. Lett. **81**, 2154 (2002).
[14] Y. Arakawa, IEICE Trans. Electron. **E85C**, 37 (2002).
[15] S. Grosse, J. H. H. Sandmann, G. von Plessen, J. Feldmann, H. Lipsanen, M. Sopanen, J. Tulkki, and J. Ahopelto, Phys. Rev. B **55**, 4473 (1997).
[16] I. V. Ignatiev, I. E. Kozin, S. V. Nair, H. W. Ren, S. Sugou, and Y. Masumoto, Phys. Rev. B **61**, 15633 (2000).
[17] P. Boucaud, K. S. Gill, J. B. Williams, M. S. Sherwin, W. V. Schoenfeld, and P. M. Petroff, Appl. Phys. Lett. **77**, 510 (2000).
[18] U. Bockelmann and T. Egeler, Phys. Rev. B **46**, 15574 (1992).
[19] U. Bockelmann, Phys. Rev. B **48**, 17637 (1993).
[20] J. Urayama, T. B. Norris, J. Singh, and P. Bhattacharya, Phys. Rev. Lett. **86**, 4930 (2001).
[21] T. Kitamura, R. Ohtsubo, M. Murayama, T. Kuroda, K. Yamaguchi, and A. Tackeuchi, Phys. Status Solidi C **0**, 1165 (2003).
[22] L. Jiang and L. V. Asryan, IEEE Photon. Technol. Lett. **18**, 2611 (2006).
[23] S. L. Chuang, *Physics of Photonic Devices*, 2nd ed. (Wiley, New York, 2009).
[24] P. S. Zory, *Quantum Well Lasers* (Academic Press, Boston, 1993).
[25] L. A. Coldren and S. W. Corzine, *Diode Lasers and Photonic Integrated Circuits* (Wiley, New York, 1995).
[26] L. V. Asryan and R. A. Suris, Semicond. Sci. Technol. **11**, 554 (1996).
[27] L. V. Asryan and R. A. Suris, Appl. Phys. Lett. **74**, 1215 (1999).
[28] L. V. Asryan, M. Grundmann, N. N. Ledentsov, O. Stier, R. A. Suris, and D. Bimberg, J. Appl. Phys. **90**, 1666 (2001).